Applied Energy 174 (2016) 108–117

Contents lists available at ScienceDirect

Applied Energy

journal homepage: www.elsevier.com/locate/apenergy

A comparative study between a Rankine cycle and a novel intra-cycle based waste heat recovery concepts applied to an internal combustion engine

Robert Morgan, Guangyu Dong *, Angad Panesar, Morgan Heikal

School of Computing, Engineering and Mathematics, University of Brighton, BN2 4GJ, United Kingdom

HIGHLIGHTS

- Concept of intra-cycle waste heat recovery (ICWHR) is proposed.
- ICWHR is compared to Rankine cycle based WHR.
- Key advantages of ICWHR are analysed.

ARTICLE INFO

Article history:
Received 9 December 2015
Received in revised form 2 April 2016
Accepted 6 April 2016
Available online 26 April 2016

Keywords:
Intra-cycle waste heat recovery
Rankine cycle
Quasi-isothermal compression
Heat recuperation
Thermal efficiency

ABSTRACT

A novel intra-cycle waste heat recovery (ICWHR) methodology, applied to an internal combustion engine is presented in this study. Through a split type thermodynamic cycle design, quasi-isothermal compression of the charge air and isobaric combustion of the air/fuel mixture can be performed separately in two chambers. Within such a design, the exhaust heat can be recovered to the intake air flow between the compression chamber and combustion chamber. Consequently, the recovered energy can be re-utilized in the combustor directly, and an intra-cycle waste heat recovery process can be achieved. To investigate the fundamental aspects of this new methodology, a comparative study between the conventional Rankine based WHR and the new ICWHR was undertaken. Both theoretical and numerical analysis were applied to evaluate the performance characteristics of these two technologies. The ICWHR cycle differs from the Rankine cycle in that an energy conversion subsystem is not necessary since the recovered energy is sent back to the combustion chamber directly, and then the system efficiency is improved significantly. Furthermore, the theoretical results indicate that the full cycle efficiency of ICWHR system is determined by the regeneration effectiveness, the compression ratio and the fuel equivalence ratio, then the limitations of Rankine cycle, such as working fluid selection and system parameter calibration can be avoided mechanically. Finally, through a one dimensional system model, analysis of optimal operation range, system efficiency and the heat transfer behaviours of ICWHR system are discussed in this paper and comparisons made with a Rankine cycle WHR system.

1. Introduction

The internal combustion (IC) engine remains the powertrain of major choice for road transport applications globally [1–3]. Concerning the energy balance of IC engines, up to 55% of the input energy is lost to the environment through the exhaust and various heat exchange processes between the engine structure, charge air and lubricating oil [4,5]. Therefore, recovering this waste heat and converting it to useful work is an obvious method of improving the overall efficiency of the combustion engine [6,7]. However, although the quantity of energy available for recovery is significant, the quality of much of the available thermal energy is low [8]. Fig. 1 shows the energy balance for a typical heavy duty diesel engine, of the type installed in a commercial vehicle. It can be seen that about 1/3 of the total energy is emitted out through the exhaust system and more than 20% is emitted out through the cooling system. Table 1 presents the typical quantities and qualities of available heat relative to ambient conditions (15 °C) normalised by the break power of the engine based on a 12.8 l Euro 6 engine described in [9]. From the table it is apparent that the heat from the vehicle cooling system and charge air cooler is of

* Corresponding author.
E-mail address: G.Dong@brighton.ac.uk (G. Dong).

http://dx.doi.org/10.1016/j.apenergy.2016.04.026
0306-2619/

Nomenclature

atdc	after top dead center
AFR	air fuel ratio
BSFC	brake specific fuel consumption (g/kW h)
C	isothermal index
CA	crank angle
CR	compression ratio
c_p	specific heat under constant pressure
c_v	specific heat under constant volume
ER	expansion ratio
h	enthalpy (kJ/kg)
int	intake
k	isentropic exponent
m	mass
Q_{LH}	fuel heat release amount (kJ)
Q_{RE}	recuperated heat (kJ)
Q_{REJC}	heat rejected during compression stage
Q_{REJC}	heat rejected during expansion stage
T	temperature (K)
tri	trilateral cycle
S	entropy
u	heat transfer coefficient

Greek symbols

γ	specific heat ratio
δ	regenerator effectiveness
η	thermal efficiency

Subscripts

1–4, 2′	stage point
Exh	exhaust
wf	working fluid
he	heat exchanger
cov	conversion efficiency
source	heat source

insufficient quality to merit effective recovery. As such, only heat from the exhaust will be considered.

Today, the thermal energy rejected to the environment from the vehicle exhaust can be recovered by a range of methods including:

- Expansion of hot exhaust gases through turbo-compounding [10].
- Recovery of heat through thermo-electric generation [11].
- Recovery of heat through a separate Rankine/organic Rankine cycle loop [12–14].

These and other methods were reviewed by Sprouse and Depcik [15] and the merits and de-merits for vehicle applications were thoroughly discussed. The review indicated that these approaches have a common feature when they are applied for IC engine waste heat recovery in that an additional energy conversion facility, such as a turbine, an expander or a thermo-electric generator (TEG) is normally to convert the thermal energy into the dynamic energy or electricity. Such a feature leads to a poor efficiency when applied on IC engines. For example, Organic Rankine Cycle (ORC), which has been proven to be one of the most effective solutions for engine waste heat recovery [16], will only provide a 3–6% engine efficiency improvement on a practical heavy duty diesel engine. This is mainly because of the mismatch of the working fluid and the highly variable exhaust temperature conditions. For the turbo-compounding system, the exhaust back pressure can be increased when the turbine is installed in the exhaust pipe. Then the waste heat recovery efficiency could be undermined because of the pumping losses and the underutilisation of the exhaust heat. Concerning the TEG system, the thermal efficiency is low because of the ineffective thermal-electrical energy conversion process [17].

Rather than using an additional system to achieve the energy conversion, directly recovering the thermal energy back into the internal combustion engine cycle, such as in a recuperated Brayton cycle, will potentially offer a higher thermal efficiency and a simpler system [18]. Roux et al. [19] reported that an 8–15% efficiency improvement can be achieved when the recuperation is applied in a Brayton cycle based gas turbine. However, a further efficiency improvement is difficult to achieve since the temperature difference between the after-compression and the after-expansion temperature of the working fluid is normally small and the amount of the recuperated heat is reduced [20].

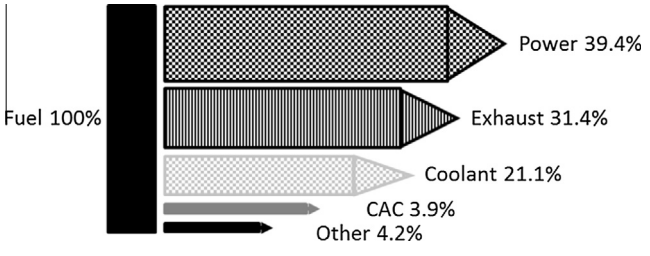

Fig. 1. Typical energy balance of a Euro 6 diesel engine [9].

Table 1
Quantities and qualities normalised to the break power.

	Quantity	Quality (exergy)
Radiator	53.5%	12.8%
Charge air cooler	9.8%	3.3%
Exhaust post turbine and aftertreatment	79.5%	59.3%

Recently, the isothermal compression technique was extensively investigated by several academic/research groups [21,22]. Isothermal compression has the potential to reduce the after-compression temperature of the working fluid. By injecting the coolant media (such as liquid nitrogen or water) into the working fluid, the temperature of the compressed working fluid can be decreased significantly, much lower than the after-expansion temperature of the working fluid. Accordingly, the amount of the recuperated heat will increase.

Applying the isothermal compression on the Diesel engines, the concept of intra-cycle waste heat recovery (ICWHR) is developed in the present work. Through a split cycle engine structure design, the compression and expansion processes are conducted in separate chambers [21,23], and then a heat recuperation is achieved through a recuperator installed between the two chambers. Due to the isothermal compression of the charge air, the temperature difference between the compression and expansion chamber is enlarged. Consequently, a significant engine efficiency improvement is achieved.

In this paper, a comparative study between the conventional Rankine cycle based WHR and the above mentioned intra-cycle waste heat recovery is conducted. For the first time, the ICWHR, which potentially leads to a step engine efficiency improvement, is demonstrated. Additionally, the application of a bottoming cycle to a conventional diesel powertrain – or 'combined cycle' is also described. Such an approach has been presented by others [24], but here, a theoretical analysis is presented together with full cycle

simulation to facilitate comparison with other options. A fundamental analysis of the two cycles is presented and compared with the Diesel internal combustion cycle to identify the ultimate potential and sensitivity to the key engine parameters such as compression ratio. Rigorous cycle analysis is then used to determine the practical efficiency of the two cycles, compared to a baseline commercial vehicle diesel engine. The paper concludes with a critical review of the two proposed cycles.

2. Thermodynamic cycle analysis of the two WHR solutions

The essential mechanism difference between ICWHR system and the conventional combined cycle WHR approach are illustrated in Fig. 2. As for an engine fitted with a Rankine WHR system, the waste heat in the exhaust flow is recovered by a recuperator, and then converted into mechanical power through the expansion of the working fluid in the turbine. Hence, the acquired power from the waste heat is decided by: (1) the heat recuperating efficiency of the heat exchanger η_{he} and (2) the energy converting efficiency of the Rankine cycle η_{cov}. Constrained by the working fluid properties and the components performance, the η_r value is normally low. However, the engine with ICWHR system has separate compression and combustion cylinders. Through a recuperator between the two chambers, waste heat can be recovered and transferred back to the combustion cylinder directly. Quasi-isothermal compression of the charge air in the compression cylinder increases the temperature difference between the compression cylinder discharge and exhaust gas. Exhaust heat is therefore more effectively recovered within the cycle. A detail description of the two WHR methods will be discussed in the following sub-sections.

2.1. Theoretical process of the ICWHR thermodynamic cycles

The split cycle engine differs from a conventional engine in that the compression and combustion processes occur in different cylinders. The basic thermodynamic of the split cycle were comprehensively described by Dong et al. [25]. The system structure and the T–S operating diagram are presented in Fig. 3a and b respectively. The stages of the cycle are as follows:

1–2′ quasi isothermal compression in the charge air in a compression cylinder.
2′–2 intra cylinder recuperation, recovering exhaust heat.
2–3 heat addition at constant pressure in the combustion cylinder.
3–4 adiabatic expansion, recovering work in the combustion cylinder.

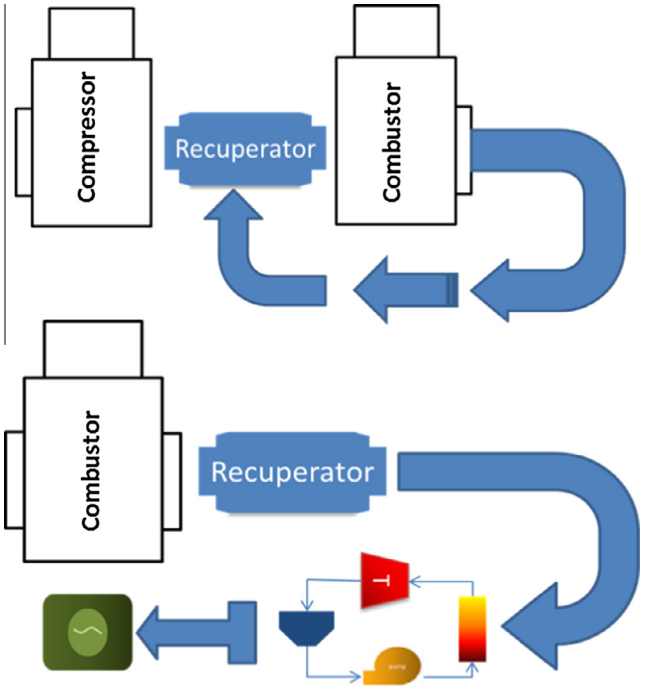

Fig. 2. Energy flow demonstration of two type WHR methodologies.

The isothermal compression process can be readily achieved through the injection of water droplets during the compression stroke [22]. Through the heat transfer between the intake air and the water spray droplets, the air temperature at the end of the compression stage can be decreased. Accordingly, the inlet temperature of the recuperator will be much lower and the recuperation efficiency improved. The temperature of the $T_{2'}$–T_4 can be calculated based on each thermodynamic process and expressed as:

$$\begin{aligned} T_{2'} &= T_1 \cdot CR^{(k-1)\cdot C} \quad T_3 = T_2 + Q_{LH}/c_p \\ T_2 &= T_{2'} + Q_{RE}/c_p \quad T_4 = T_3/CR^{(k-1)} \end{aligned} \tag{1}$$

Accordingly, the thermal efficiency of split cycle can be described as:

$$\begin{aligned} \eta = \frac{(Q_{LH}+Q_{RE})-(Q_{REJC}+Q_{REJE})}{Q_{LH}} &= \frac{CR^{(k-1)}}{CR^{(k-1)}-\delta} \\ &+ \frac{c_p \cdot T_1}{Q_{LH}\cdot(CR^{(k-1)}-\delta)} \cdot \begin{bmatrix} 2\cdot\delta\cdot CR^{(k-1)\cdot C} - \delta\cdot CR^{(k-1)\cdot C+1} \\ -CR^{(k-1)}\cdot C + CR^{(k-1)} - \delta \end{bmatrix} \\ &- \frac{c_v \cdot T_1}{C\cdot Q_{LH}}\left(CR^{(k-1)\cdot C}-1\right) \end{aligned} \tag{2}$$

Here, T_1 is the initial temperature of intake air, and the specific heat ratio of air is a constant K. The compression ratio and expansion ratio are CR and ER respectively. The parameter C $(0 \leqslant C \leqslant 1)$ is the isothermal index which represents the deviation of the compression process towards an isothermal process. Normally the value of C is 0 when the compression process is an isothermal process. The compression tends to the adiabatic case when C is closer to 1. The recuperation effectiveness δ $(0 \leqslant \delta \leqslant 1)$ represents the recuperating efficiency. The Q_{REJC} and Q_{REJE} are the heat rejected during the compression and expansion stroke respectively. The detail of the above thermodynamic analysis can be found in reference paper [25].

The efficiency of split cycle engine is determined by 4 key factors; the compression/expansion ratio, the recuperation effectiveness and the heat release amount from the fuel. This is different from the ideal engine efficiency, which is dominated by the compression ratio alone. In the following section, the influencing mechanism of these factors will be discussed. Based on the analysis result, the system design principles of split cycle engine will be studied.

2.2. Theoretical analysis of the maximum efficiency of the combined cycle

The combined cycle concept consists of a conventional diesel engine combined with a Rankine cycle to recover waste heat. As such, the impact of waste heat recovery on the system efficiency can first be determined by considering the Rankine cycle in isolation. Referring to Fig. 4, the maximum work that can be recovered from two temperature sources is defined by the Carnot cycle limits. However, in the case of waste heat recovery from a vehicle exhaust system, the heat source is finite and will vary through the recovery process. As such, the trilateral cycle provides a more realistic

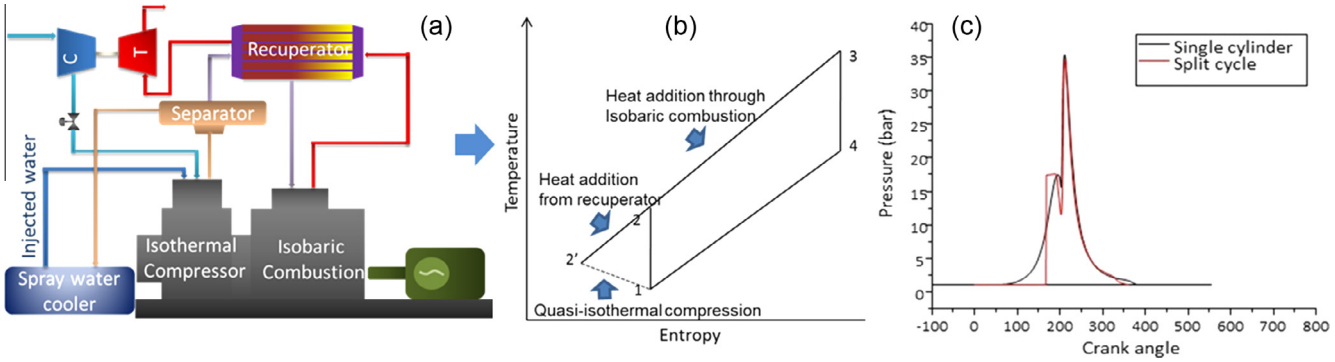

Fig. 3. System structure and typical operating features of split cycle with ICWHR.

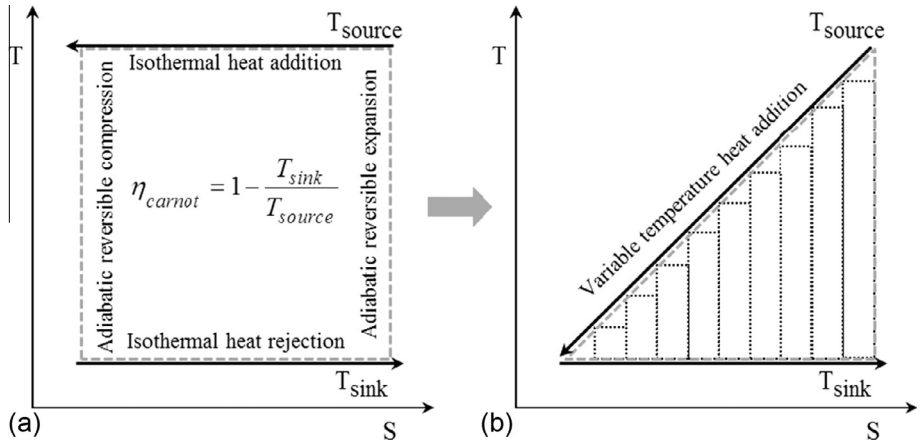

Fig. 4. T–S diagram evolution from infinite source and sink to finite source: (a) Carnot cycle and (b) trilateral cycle.

assessment of the ultimate efficiency of the Rankine part of the combined cycle, described by Eq. (3) [24].

$$\eta_{tri} = 1 - \frac{T_{sink}\ln\left(\frac{T_{source}}{T_{sink}}\right)}{T_{source} - T_{sink}} \tag{3}$$

The source temperature can be determined using constant pressure air standard cycle analysis [26], relating the compression ratio and heat addition, based on the lower heating value:

$$T_{source} = (T_1 \cdot CR^{k-1} + Q_{LH}/c_p)/CR^{k-1} \tag{4}$$

Combining Eqs. (3) and (4), it can be achieved that:

$$n_{tri} = 1 - RgT_1 \ln\left[\frac{(1 + ET_1CR^{k-1})}{CR^{k-1}} \cdot (CR^{k-1} + E)^{1/k-1}\right] \tag{5}$$

The maximum efficiency of the combined cycle therefore depends on the compression ratio of the engine and heat addition. The

Table 2
Comparison of the 4 typical thermal dynamical cycles.

	Brayton cycle	Split cycle with quasi iso-thermal compression	Rankine cycle with maximum available waste heat	Typical practical Rankine cycle
	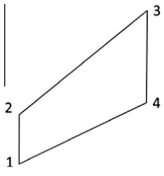	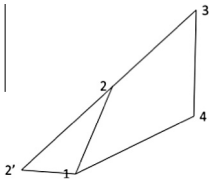	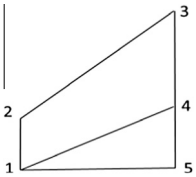	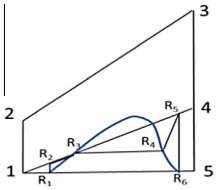
Efficiency	$\eta_t = 1 - \frac{1}{CR^{k-1}}$	$\eta_t = 1 - \left[\frac{CR^{(k-1)\cdot C-1} - F(1-\frac{1}{CR^{(k-1)}})+}{\frac{c_v}{C\cdot c_p}(CR^{(k-1)\cdot C}-1)}\right] \Big/ E$ $E = (Q_{LH})/(c_p \cdot T_1)$ $F = (Q_{RE} + Q_{LH})/(c_p \cdot T_1)$	$\eta_t = 1 - RgT_1 \ln\left[\frac{\left(1 + ET_1CR^{k-1}\right)}{CR^{k-1}} \cdot (CR^{k-1} + E)^{1/k-1}\right]$ $E = (Q_{LH})/(c_p \cdot T_1)$	$\eta_{conversion} = \eta_{thermal}\eta_{recovery}$ $= \frac{\dot{W}_{net}}{\dot{Q}_{in}}\frac{\dot{Q}_{in}}{\dot{Q}_{max}} = \frac{\dot{W}_{net}}{\dot{Q}_{max}}$ $\dot{W}_{net} = \eta_{transmission}(\dot{W}_{expander} - \dot{W}_{pump})$ $-\dot{W}_{backpressure+fan.power}$ $-\dot{W}_{control+machine.cooling}$ $W_{backpressure+fan.power} = 0.003\dot{Q}_{HEX}^{1.3}$
WHR available range	–	$T_4 > T_2'$	$T_4 > T_1$	$T_4 > T_1$

maximum efficiencies of the combined and split cycle engines are compared with the conventional Brayton cycle. As shown in Table 2, the efficiency of the internal combustion engine can be expressed as a function of the compression ratio (CR) and ratio of the specific heats (k):

$$\eta_{ideal} = 1 - \frac{1}{CR^{k-1}} \tag{6}$$

Inspection of Eq. (6) shows the limiting efficiency of the Brayton cycle is dependent on the compression ratio only since the working fluid of the engine is air. For the split cycle and combined cycle, the recuperator effectiveness δ has an important role in the cycle efficiency. The difference is the expansion ratio, which will not affect the maximum heat recovery efficiency (HRmax) of the combined cycle. However, both the expansion ratio and the isothermal index C are crucial for the split cycle since the amount of recovered heat of this kind of engine is bounded to the engine intake air and exhaust temperature.

The ideal Brayton, practical split cycle and combined cycles, are compared in Table 2. As mentioned in the above analysis, the maximum heat recovery efficiency of the combined cycle only indicates the potential of the engine with Rankine based WHR system. Its practical efficiency will also be strongly affected by the energy converting efficiency of the Rankine cycle $\eta_{cov.}$ Additionally, the value of η_{cov} is very low due to the practical constraints imposed through the selected working fluid. The selection and design of the working fluid for the Rankine cycle is of considerable research interest. The analysis of the practical Rankine cycle will be analysed in the next section.

The temperature of the exhaust side (represented by T_4) and ambient side (represented by T_1) are theoretically the same for both the split cycle and combined cycle engine. However, the ideal cycle efficiency can be significantly different for the two cycles. Giving a fixed condition of Q_{LH} = 1700 J/cycle and δ = 0.88, the efficiency difference of the cycles under different CR conditions is shown in Fig. 5(a). Here an iso-thermal index C of 0.87 is used for the split cycle analysis. It can be seen that the efficiency of both these two cycles are much higher than that of Brayton cycle. However, the efficiency of the split cycle is slightly higher, especially under lower CR conditions. To illustrate such a result, a temperature–entropy analysis is shown in Fig. 5(b). The figure clearly shows that the application of intra-cycle recuperation will affect the original engine operating parameters. The recuperated heat enables an increment of the temperature T_2 in the split cycle case, and then makes it higher than that in combined cycle case. As a result, the whole cycle efficiency of the split cycle becomes higher. The figure also shows that the efficiency of the split cycle can be improved when a suitable over expansion ratio is applied on the split cycle engine.

The above analysis indicates the potential of both split cycle and combined cycle is higher than the conventional Brayton cycle. The efficiency variations of the split cycle and combine cycle under different δ and CR conditions are shown in Fig. 6(a) and (b) respectively. It can be seen that the overall efficiency of split cycle is noticeable higher, especially under low CR conditions. Also, it can be seen that the efficiency of split cycle benefits more from the increment of recuperation effectiveness value δ. However, the practical efficiency of split cycle is much closer to the theoretical result comparing to the combined cycle because the energy conversion efficiency η_{cov} of Rankine cycle is relatively low. The detail analysis of the practical efficiencies of these two WHR systems will be discussed in the following section.

3. Performance analysis of intra-cycle based and combined cycle based WHR methodology

The theoretical analysis presented in Section 2, although useful in comparing different cycle concepts does not account for the practical losses in implementing the cycle in a heavy goods vehicle. Full cycle analysis is required to assess the full performance potential of the combined and split cycles, compared to a conventional diesel engine.

For comparing the performances of the intra-cycle and combined cycle based WHR systems in detail, a hybrid modelling methodology was applied in this section. The architecture of the modelling work can be seen in Fig. 7. Through the LMS Imagine. Lab AMESim [27,28] software, a one-dimensional baseline engine model, and a split cycle engine model were developed. The IFP engine system model in AMEsim is in particular devoted to the development of internal combustion engine models. The detail of the model construction and validation can be seen in reference paper [25]. Furthermore, the Aspen HYSYS [29] software was applied to build the recuperator model for split cycle engine, and the heat exchanger model for combined cycle. The validation of the recuperator/heat exchanger model can be seen in reference paper [23,25]. Finally, through coupling the AMEsim based engine models and the HYSYS based recuperator/heat exchanger models, the system efficiency of the split cycle and the combined cycle can be compared based on a proposed baseline engine specifications.

The OM471 engine, which was used in previous WHR research [24], was used as the baseline engine in this paper. The engine is a

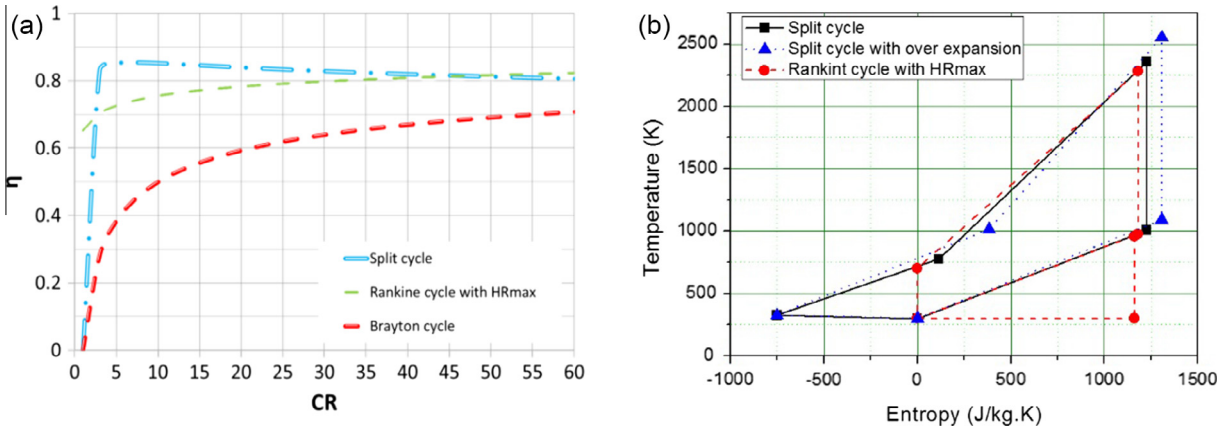

Fig. 5. Comparison of (a) thermal efficiencies (a) and (b) T–S diagrams.

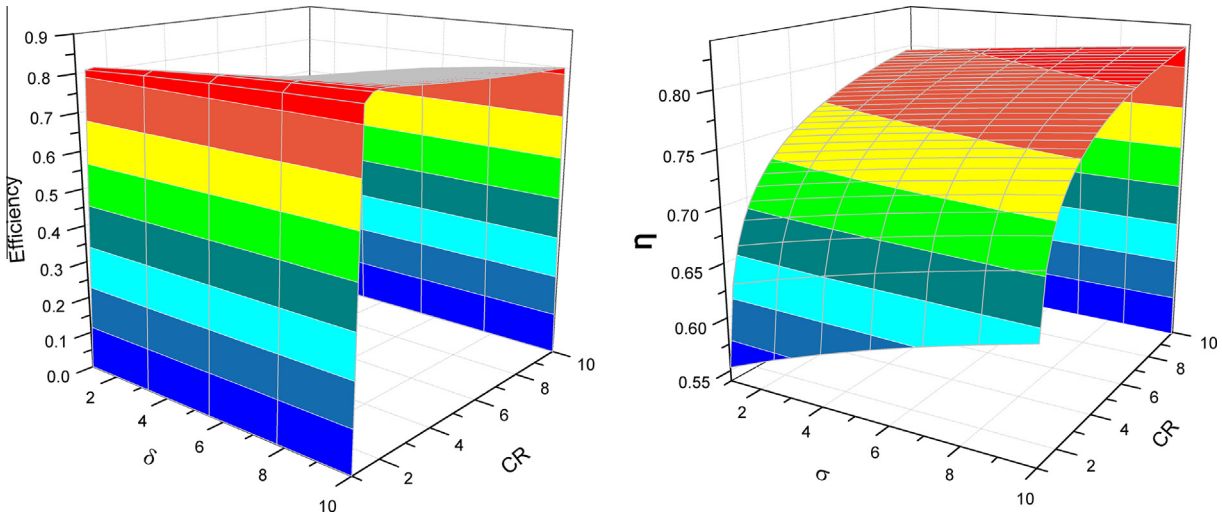

Fig. 6. Thermal efficiencies of (a) split cycle and (b) combined cycle.

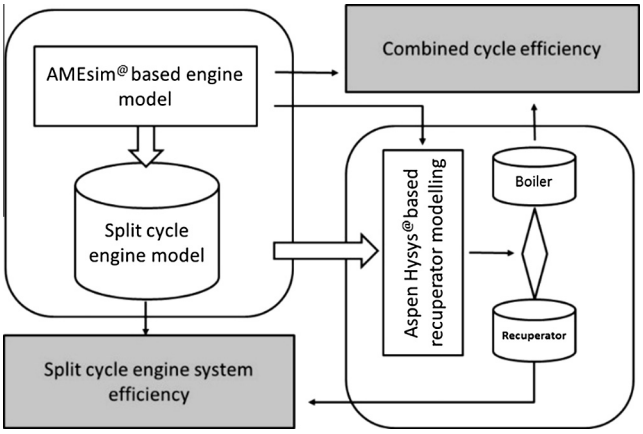

Fig. 7. Architecture of the thermodynamic cycle modelling solution.

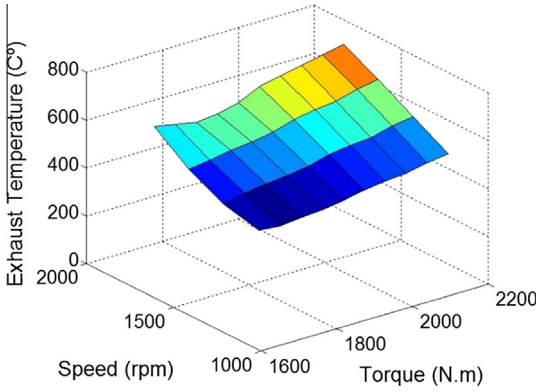

Fig. 8. The exhaust temperature map of the test engine.

12.8-l straight-six engine which achieve the Euro VI emission standard. A map of the exhaust temperature as a function of engine speed and torque is shown in Fig. 8. The map is calculated through the above one-dimensional model, and the engine model is validated against the experimental results from single cylinder engine testing. This engine utilized a high efficiency SCR for NOx emissions control. The exhaust heat was calculated after the turbine, DPF and SCR components. The exhaust lines were considered non-insulated and a 25 °C temperature drop was considered over the after-treatment devices. A representative test point at rated power and nominal torque was selected, as presented in Table 3. Then the system efficiencies of the ICWHR and the combined cycle are compared. The specifications of the baseline engine and the split cycle engine, along with the configurations of the combined cycle WHR system, are shown in Table 3 as well. For the split cycle engine, 3 cylinders of the total 6 are modified for isothermal compressor, and the other 3 are designed as combustors. In the isothermal compressors, water was used as the cooling media to control the air temperature during the compression process. For the recuperator between the compressor and combustor, the exhaust was inlet in the opposite direction of the intake fresh air to maximum the recuperation efficiency.

For the combined cycle, the selection of a suitable working fluid is the first and the most important step in maximising the system performance. Previous study indicate that the organic working fluid for vehicle WHR system normally favour of a heat source quality of <400 °C due to molecular weight, thermal decomposition and heat transfer irreversibility considerations. For the non-organic working fluids like water, a heat source quality >500 °C is needed due to the large latent heat [30]. To meet the complex requirements for automotive applications, binary water blends may present an alternative avenue. As a result, a binary water blend with 50% water and 50% ethanol blend was selected to reach the maximum efficiency of the combined cycle, and then the configurations of the sub-components were set accordingly.

Based on the above modelling configurations and parameter selections, a comparison of combined cycle and an intra-cycle based waste heat recovery methodology becomes possible based on the practical engine operation conditions.

3.1. Comparison of the heat recuperating efficiency η_{he} from the two systems

As discussed in Section 2, the total efficiency of a combined cycle WHR system is decided by; (1) the heat recuperating efficiency of the heat exchanger η_{he} and (2) the energy converting efficiency of the combined cycle η_{cov}. For both a split cycle engine and the combined cycle, the waste heat are harvested with the same mechanism; heat transfer between exhaust flow and working fluid within the recuperator/evaporator system. For the split cycle engine, the working fluid is the compressed intake air in the recuperator, thus the intake air mass flow rate and the heat

Table 3
Specifications of the baseline engine, the split cycle engine and the combined cycle WHR system.

Base engine specifications
- Cylinder number = 6
- AFR = 23:1
- *CR* = 17 (adjustable)
- Bore [mm] = 128
- Stroke [mm] = 148
- Engine speed [rpm] = 1800
- Target power [kW] = 327
- Indicated thermal efficiency η_{th} = 39.4%

Split cycle engine specifications:(3 compressors and 3 combustors for split cycle engine)
Isothermal compressor:
- Cooling media: water
- Cooling temperature: 50 °C
- Injection pressure: 600 bar

Recuperator:
- Total length = 600 mm
- Number of tubes = 70
- Tube inner diameter = 2 mm
- Shell diameter = 35 mm
- Exhaust inlet location relative to intake: opposite side

Combined cycle WHR system Working fluid
- 50% water 50% ethanol (by mass)

Heat exchanger (combined cycle)
- $T_{maxf\ luid}$ = 300 °C
- ΔP_{fluid} = 0.5 bar
- $T_{pinch\ point\ HEX}$ = 15 °C

Expansion machine and pump
- $\eta_{expansion}$ = 70%
- Expansion ratio = 2-stage, 6:1 each (max)
- η_{pump} = 60%
- $\eta_{transmission}$ = 93%

Air condensed temperature
- $T_{coolant\ air}$ = 50 °C

recuperation performance will vary under different engine operating conditions. Fig. 9(a) shows the one dimensional temperature distributions of the exhaust flow and the intake air in the recuperator calculated for the split cycle engine. It can be seen that the exhaust temperature increases when a lower compression ratio (*CR*) is applied. However, the corresponding temperature increase of the intake air is not as high as for the exhaust temperature. The modelling results shown in this figure indicate that the exhaust/intake air temperature difference is increased under low *CR* conditions, and then the recuperation performance becomes poorer accordingly.

Maintaining the compression ratio at the original value of 17, the one dimensional temperature distribution within the evaporator applied in combined cycle is shown in Fig. 9(b). Within the evaporator, the compressed water/ethanol mixture is evaporated and the mixture outlet temperature increased to 583 K and the exhaust flow was cool down to 381 K, which is slightly lower than the case on split cycle engine (423 K@*CR* = 17). The recuperator outlet temperature is therefore much lower comparing to the cases on split cycle engine.

Normally for a recuperator/heat exchanger, a recuperation effectiveness δ can be defined to evaluate the heat recovery efficiency [25], as:

$$\delta = \frac{T_{WFI} - T_{WFO}}{T_{ExhI} - T_{WFO}}$$

Here, T_{ExhI} is the inlet temperature of the heat source flow, T_{WFI} and T_{WFO} are the inlet and outlet temperature of the working fluid respectively. Due to the large latent heat of evaporation and heat capacity of the water/ethanol mixture, the working fluid outlet temperature of the evaporator is relatively low comparing to that on split cycle engine. Based on the definition of δ, it can be concluded that the calculated recuperation effectiveness δ of the evaporator for the combined cycle is lower than that of the recuperator on the split cycle engine due to the lower working fluid outlet temperature. However, the exhaust flow outlet temperature of the evaporator is 381 K which is comparable to that for split cycle engine cases. This phenomenon indicates that the total amount of heat recovered from the exhaust flow are similar between the case for combined cycle and split cycle.

To evaluate the heat recovery effectiveness of the two cycles for a given value of δ, the heat recuperating efficiency – $\eta_{he} = \left|\frac{\Delta Eth_{WF} * \dot{m}_{wf}}{\Delta Eth_{Exh} * \dot{m}_{Exh}}\right|$, was defined for the comparison of the heat recovery process in these two cycles. Here ΔEth_{WF} is the specific enthalpy increment of the working fluid, and ΔEth_{Exh} is the specific enthalpy decrement of the exhaust flow $\dot{m}_{wf}$ and $\dot{m}_{Exh}$ are the mass flows of the working fluid and exhaust respectively. Based on the system configurations and parameters listed in Table 3, the comparison of the percentage of exhaust heat recovered from both the recuperator on split cycle engine and the heat exchanger for combined cycle are compared under different exhaust inlet temperature conditions. As can be seen in Fig. 10, the recovered heat from the evaporator is about 5% higher than the recuperator when the exhaust temperature T_{exh} is 949 K (*CR* = 17), however these two values converge when T_{exh} decreases. This analysis indicates that the heat recuperating efficiency η_h of the evaporator for combined cycle can be slightly higher than that of the recuperator for split cycle engine given the same exhaust flow conditions.

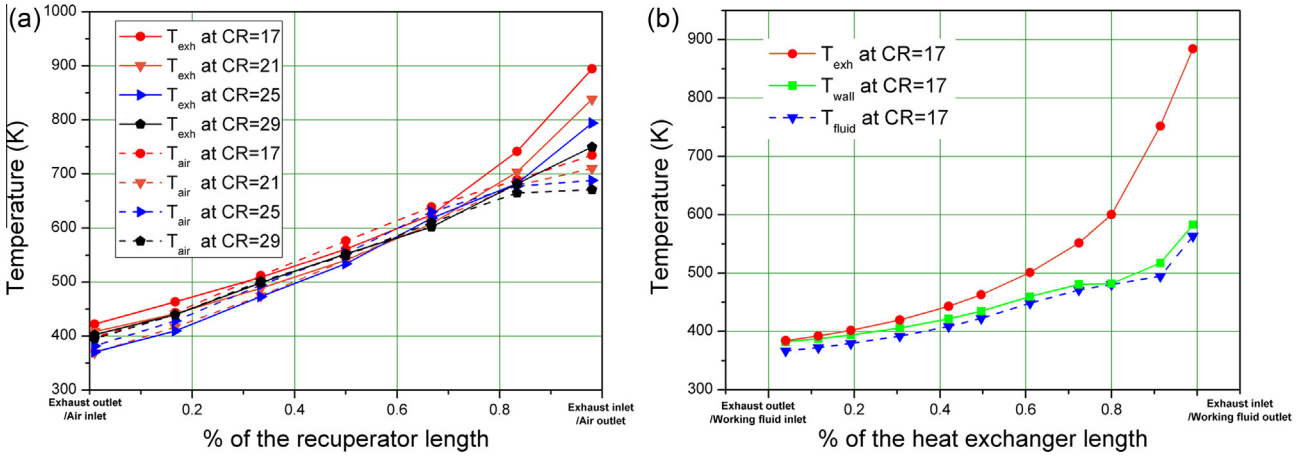

Fig. 9. The one-dimensional temperature distribution in (a) recuperator (for split cycle) and (b) heat exchanger (for Rankine cycle).

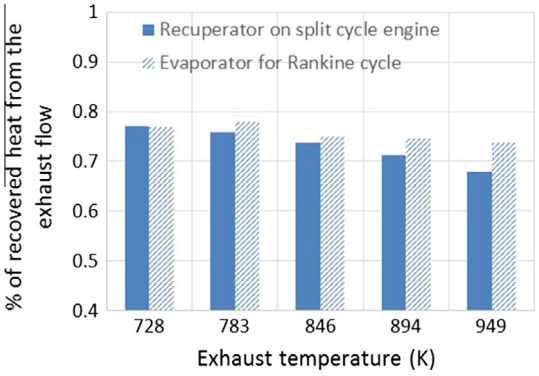

Fig. 10. Comparison of the recovered hear between the split cycle and combined cycle.

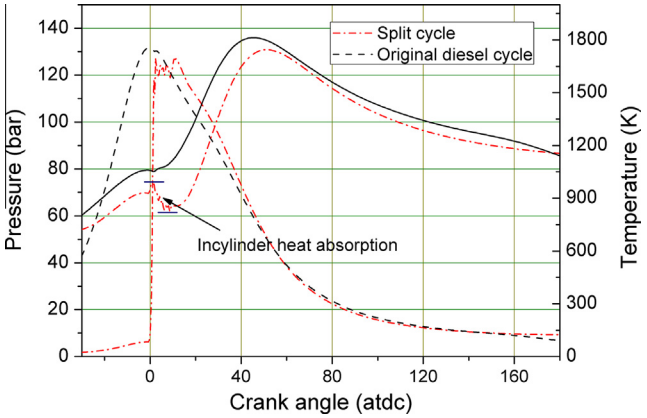

Fig. 12. In-cylinder combustion process of split cycle engine and the original diesel engine.

3.2. Comparison of the energy converting efficiency η_{cov} of the two systems

Assuming a fixed heat recuperating efficiency η_{he}, the discussion in Section 2 indicates that the final thermal efficiency of a heat recovery system is decided by the energy converting process which convert the recovered heat to the work output. Thus, the energy converting efficiency η_{cov} of split cycle and Rankine cycle is compared in this section.

Keeping the compression ratio $CR = 17$, the T–S operating diagrams of both split cycle and combined cycle are shown in Fig. 11(a) and (b) respectively. On the split cycle engine, the compressed intake air acts as the thermal media to absorb the heat from the exhaust flow. In the quasi-isothermal compression process, the intake is mixed with the injected water in the compression cylinder. The water temperature can be kept close to ambient temperature by the rejection of heat to the environment post recovery and pre injection to the compressor cylinder. Hence the intake air temperature increases only slightly from 303 K to 343 K during the compression process, and then was heated up to 752 K in the recuperator, as can be seen in Fig. 11(a). After the heat recuperation process, the heated high pressure air was induced into the combustion chamber, which then triggers the auto ignition of the air–fuel mixtures. On the T–S diagram, the area between the compression line and the heat recuperation line represents the recovered energy from the exhaust. According to the definition of the Carnot cycle thermal efficiency: $\eta_{th} = 1 - \frac{T_L}{T_H}$, it can be deduced that the energy converting efficiency η_{cov} of split cycle is decided by the average intake air temperature during the compression process which represent the T_L, and the average temperature during the recuperation process which represent the T_H. The calculation result base on the above T–S diagram shows that the η_{cov} of split cycle is 52%.

Keeping the same condition of $CR = 17$, the T–S diagram of the combined cycle is shown in Fig. 11(b). In the combined cycle, the working fluid is the mixture of water and ethanol with the identical mass friction of 50%. A maximum cycle pressure of 58 bar was considered optimal, since this corresponded to a pressure ratio in a two-stage expansion machine that can be achieved by both piston expanders and radial turbines [24,31]. The analysis in Section 3.1 indicated that the heat recuperating efficiency η_{he} for combined cycle is 5% higher than that of the split cycle under this condition. However, due to the latent heat during the liquid–gas phase transition process and the high specific heat capacity of the working fluid, the final working fluid temperature of the combined cycle is 543 K, which is much lower than the split cycle case. On the other hand, to guarantee the working fluid is kept in the gas phase after the expansion process in the turbine, and to reduce the waste recovery system cost, the working fluid temperature is cooled down to 365 K by the engine coolant water in the condenser. According to the Carnot cycle based thermal efficiency analysis mentioned above, it can be calculated that the energy conversion efficiency η_{cov} of combined cycle is 12.1% which is much lower than the case on split cycle engine.

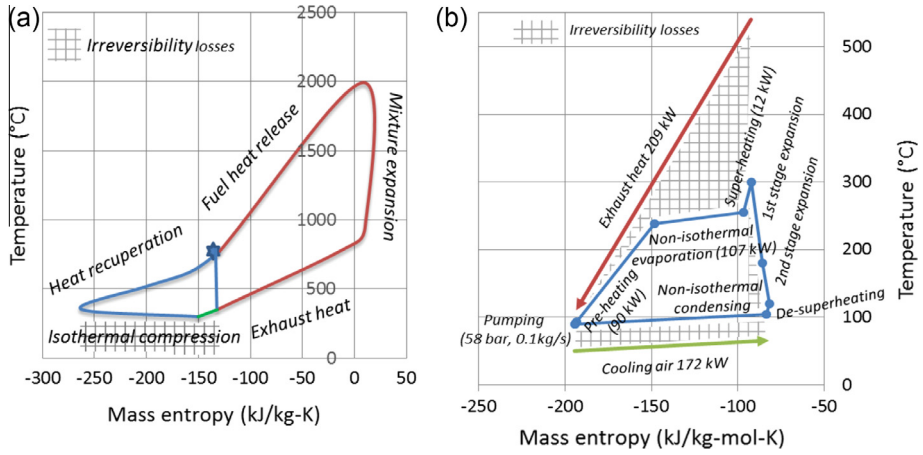

Fig. 11. Energy converting efficiency analysis based on the temperature–entropy diagram of (a) split cycle and (b) Rankine cycle.

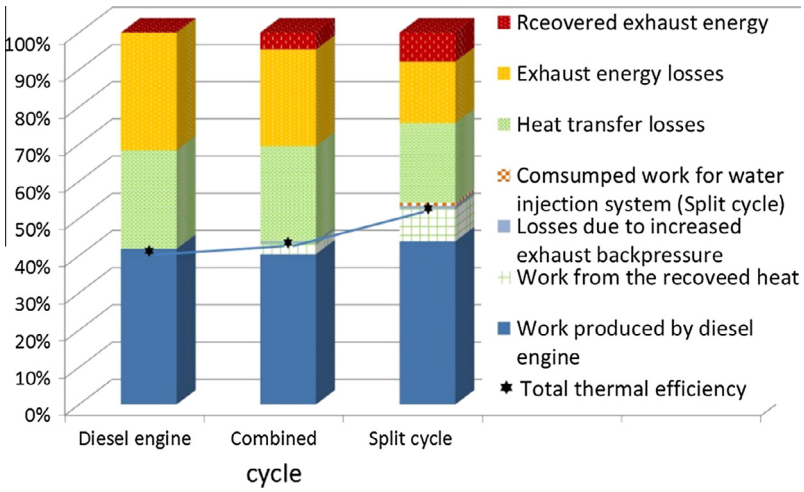

Fig. 13. Energy distribution of original diesel cycle, split cycle and combined cycle applied on the diesel engine.

3.3. Full cycle thermal efficiency comparison between the two systems

As introduced in Section 2, the Rankine cycle based WHR system is a kind of passive WHR system. Thus, it can be assumed that the diesel engine efficiency will not be significantly affected by the WHR system [32]. However, for the split cycle engine it is different. As a stage of the whole thermodynamic cycle, the waste heat recuperation process occurs between the intake air compression stage and the mixture combustion stage on the split cycle engine. Obviously, the isothermal compression, the heat recuperation and the combustion process are interdependent. The isothermal compression and heat recuperation processes of the split cycle engine were illustrated on the T–S diagram in Section 3.2. However, the detail of the combustion process of it is not described. Fig. 12 shows the in-cylinder combustion pressure and temperature variations of both the split cycle engine and the original diesel engine.

On split cycle engine, the combustion occurs in the combustion cylinder chamber. After the heat recuperation, the heated intake air was induced into the combustion chamber close to top dead center. As a result, a sharp pressure rise can be seen when the intake valve is open, and the pressure fluctuations can be observed as well due to the high intake velocity. Due to the air induction process, the fuel injection timing on the split cycle engine is slightly delayed comparing to the diesel engine. Correspondingly, a nearly isobaric combustion process appears on this engine.

Due to the isothermal compression, it can be seen that the intake temperature of the split cycle engine is lower than the diesel case at the TDC position even if it is heated by the exhaust gas in the recuperator. So the in-cylinder combustion temperature will be lower than the diesel case as well. Such a low in-cylinder temperature leads to a low heat transfer losses in the combustion chamber. Since the isothermal compression is achieved by the water pumping and injection system, a 3.2 kW extra power in consumed in this system, which leads to a 0.8% thermal efficiency losses.

Based on the above analysis of the heat recuperation process and engine combustion process, the system thermal efficiency can be achieved for both split cycle and combined cycle. Fig. 13 demonstrates the energy distributions under the cases of original diesel engine, the split cycle and the combined cycle. The application of the recuperator/heat exchanger system leads to a slight increase of the exhaust back pressure, and then an extra energy losses can be seen in both the combined cycle and split cycle cases (0.5% thermal efficiency losses in combined cycle, and 0.77% efficiency losses in split cycle case). However, the system efficiency still improved through the application of these two thermodynamic cycles. Comparing to the original diesel engine with an indicated thermal efficiency of η_{th} = 40.4%, the η_{th} of combined cycle is increased to 44.2%, which demonstrate a 3.8% efficiency improvement through the Rankine cycle based WHR system (combined cycle). However, the split cycle based intra-cycle WHR method yielding a system thermal efficiency of 52.2%, which is much higher than that of the combined cycle.

4. Conclusions

A comparison study on the ICWHR system, which achieved through a novel split thermodynamic cycle design, and the conventional Rankine cycle based WHR technology (combined cycle) is conducted in this paper. Through both the theoretical and the numerical analysis, 5 major findings are achieved as follows:

(1) The theoretical analysis indicate that the upper limits of efficiency of both the split cycle and combined cycle are about 20% higher than the conventional diesel cycle. The overall efficiency of split cycle is slightly higher comparing to that of combined cycle, especially under low compression ratio conditions.
(2) Due to the large evaporation latent heat and heat capacity of water/ethanol mixture, the maximum working fluid temperature of the combined cycle is much lower comparing to that on split cycle engine. However, the heat recuperating efficiency η_{he} of combined cycle is 5% higher than that of the split cycle when the exhaust temperature T_{exh} is 949 K (CR = 17). These two values get closer when T_{exh} decreases.
(3) To guarantee the working fluid keeps in gas phase after the expansion process in the turbine, and to reduce the waste recovery system cost, the working fluid temperature is cooled down to 365 K for combined cycle case, which is much higher than that in split cycle. According to the Carnot cycle based thermal efficiency analysis, the energy conversion efficiency η_{cov} of the combined cycle is 12.1%, which is much lower than the case on split cycle engine.
(4) Due to the isothermal compression, the intake temperature of a split cycle engine is lower than the original diesel engine even it is heated by the exhaust gas in the recuperator. So the in-cylinder combustion temperature will be lower than the diesel case as well. Such a low in-cylinder temperature leads to a low heat transfer losses during the combustion process.

(5) Based on the above analysis of the heat recuperation process and engine combustion process, the system efficiencies of the combined cycle and the split cycle are achieved. The indicated thermal efficiency η_{th} of combined cycle is increased to 44.2%, which demonstrate a 3.8% efficiency improvement comparing to the original diesel cycle. However, the split cycle based intra-cycle WHR method yielding a system thermal efficiency of 52.2%, which is much higher than that of the combined cycle.

Acknowledgements

The research presented in this paper was funded by Innovate UK as part of the Crypower Project through the IDP8 technology program and EPSRC project 'Ultra Efficient Engines and Fuels' grant number EP/M009424. The authors would also like to thank LMS for providing an AMEsim licence under their academic support programme.

References

[1] Pandiyarajan V et al. Second law analysis of a diesel engine waste heat recovery with a combined sensible and latent heat storage system. Energy Policy 2011;39(10):6011–20.
[2] Di Battista D, Mauriello M, Cipollone R. Waste heat recovery of an ORC-based power unit in a turbocharged diesel engine propelling a light duty vehicle. Appl Energy 2015;152:109–20.
[3] Musculus MPB, Miles PC, Pickett LM. Conceptual models for partially premixed low-temperature diesel combustion. Prog Energy Combust Sci 2013;39(2–3):246–83.
[4] Aly SE. Diesel-engine waste-heat power cycle. Appl Energy 1988;29(3):179–89.
[5] Mavropoulos GC. Experimental study of the interactions between long and short-term unsteady heat transfer responses on the in-cylinder and exhaust manifold diesel engine surfaces. Appl Energy 2011;88(3):867–81.
[6] Kuboyama T et al. Improvement of thermal efficiency of a four-cylinder gasoline homogeneous charge compression ignition engine via blowdown supercharging. Int J Engine Res 2012;13(3):226–37.
[7] Xie H, Yang C. Dynamic behavior of Rankine cycle system for waste heat recovery of heavy duty diesel engines under driving cycle. Appl Energy 2013;112:130–41.
[8] Fu JQ et al. Energy and exergy analysis on gasoline engine based on mapping characteristics experiment. Appl Energy 2013;102:622–30.
[9] Kropiwnicki J, Kneba Z, Ziolkowski M. Test for assessing the energy efficiency of vehicles with internal combustion engines. Int J Automot Technol 2013;14(3):479–87.
[10] He G, Xie H. Fuel saving potential of different turbo-compounding systems under steady and driving cycles. SAE International; 2015.
[11] Riley PH. Affordability for sustainable energy development products. Appl Energy 2014;132:308–16.
[12] Costall AW et al. Design methodology for radial turbo expanders in mobile organic Rankine cycle applications. Appl Energy 2015;157:729–43.
[13] Richardson ES. Thermodynamic performance of new thermofluidic feed pumps for Organic Rankine Cycle applications. Appl Energy 2016;161:75–84.
[14] Macian V et al. Methodology to design a bottoming Rankine cycle, as a waste energy recovering system in vehicles. Study in a HDD engine. Appl Energy 2013;104:758–71.
[15] Sprouse C, Depcik C. Review of organic Rankine cycles for internal combustion engine exhaust waste heat recovery. Appl Therm Eng 2013;51(1–2):711–22.
[16] Song J, Gu CW. Performance analysis of a dual-loop organic Rankine cycle (ORC) system with wet steam expansion for engine waste heat recovery. Appl Energy 2015;156:280–9.
[17] Heghmanns A, Beitelschmidt M. Parameter optimization of thermoelectric modules using a genetic algorithm. Appl Energy 2015;155:447–54.
[18] Galindo J et al. Brayton cycle for internal combustion engine exhaust gas waste heat recovery. Adv Mech Eng 2015;7(6).
[19] Le Roux WG, Bello-Ochende T, Meyer JP. A review on the thermodynamic optimisation and modelling of the solar thermal Brayton cycle. Renew Sustain Energy Rev 2013;28:677–90.
[20] Sanjay, Prasad BN. Energy and exergy analysis of intercooled combustion-turbine based combined cycle power plant. Energy 2013;59:277–84.
[21] Coney MW, Linnemann C, Greenwood AL. First test results of a novel large high-efficiency reciprocating piston engine. In: Proceedings of the Fall Technical Conference of the ASME Internal Combustion Engine Division. ASME paper no. ICES2003-561(ICE-vol. 40). p. 409–18.
[22] Coney MW, Linnemann C, Morgan RE, Bancroft TG, Sammut RM. A novel internal combustion engine with simultaneous injection of fuel and pre-compressed pre-heated air. In: Proceedings of the Fall Technical Conference of the ASME Internal Combustion Engine Division, 2002. ASME paper no. ICEF2002-485(ICE-vol. 39). p. 67–77.
[23] Coney MW, Linnemann C, Abdallah HS. A thermodynamic analysis of a novel high efficiency reciprocating internal combustion engine – the isoengine. Energy 2004;29(12–15):2585–600.
[24] Panesar AS, et al. A novel organic rankine cycle system with improved thermal stability and low global warming fluids. In: ICPER 2014 – 4th International Conference on Production, Energy and Reliability, 2014. p. 13.
[25] Dong GY, Morgan R, Heikal M. A novel split cycle internal combustion engine with integral waste heat recovery. Appl Energy 2015;157:744–53.
[26] Heywood JB. Internal combustion engine fundamentals. McGraw-Hill series in mechanical engineering. New York: McGraw-Hill; 1988. xxix, 930p, 2p. of plates.
[27] Chen DG et al. A research on compressed natural gas engine fuel supply system for rapid prototyping based on AMEsim. Appl Energy Technol 2013;724–725:1317–23. Pts 1 and 2.
[28] Fang ZH, et al. Simulation of a gasoline injection system based on AMESim. In: ISTM/2007: 7th International Symposium on Test and Measurement, vols. 1–7, Conference Proceedings, 2007. p. 5409–5412.
[29] Smejkal Q, Soos M. Comparison of computer simulation of reactive distillation using ASPEN PLUS and HYSYS software. Chem Eng Process 2002;41(5):413–8.
[30] Dolz V et al. HD Diesel engine equipped with a bottoming Rankine cycle as a waste heat recovery system. Part 1: Study and analysis of the waste heat energy. Appl Therm Eng 2012;36:269–78.
[31] Shu GQ et al. Alkanes as working fluids for high-temperature exhaust heat recovery of diesel engine using organic Rankine cycle. Appl Energy 2014;119:204–17.
[32] Hossain SN, Bari S. Waste heat recovery from the exhaust of a diesel generator using Rankine Cycle. Energy Convers Manage 2013;75:141–51.